Opinion TRENDS in Biotechnology Vol.22 No.11 November 2004

Ribosomal antibiotics: structural basis for resistance, synergism and selectivity

Tamar Auerbach, Anat Bashan and Ada Yonath

Department of Structural Biology, The Weizmann Institute, 76100 Rehovot, Israel

Various antibiotics bind to ribosomes at functionally relevant locations such as the peptidyl-transferase center (PTC) and the exit tunnel for nascent proteins. High-resolution structures of antibiotics bound to ribosomal particles from a eubacterium that is similar to pathogens and an archaeon that shares properties with eukaryotes are deciphering subtle differences in these highly conserved locations that lead to drug selectivity and thereby facilitate clinical usage. These structures also show that members of antibiotic families with structural differences might bind to specific ribosomal pockets in different modes dominated by their chemical properties. Similarly, the chemical properties of drugs might govern variations in the nature of seemingly identical mechanisms of drug resistance. The observed variability in binding modes justifies expectations for structural design of improved antibiotic properties.

Ribosomes are ribonucleoprotein assemblies that catalyze the sequential polymerization of amino acids into proteins according to the genetic code. They are built of two subunits, termed the 30S and 50S subunits in prokaryotes. The small subunit provides the decoding center, whereas the large contains the peptidyl-transferase center (PTC) and the protein exit tunnel. The ribosome possesses three tRNA binding sites: the aminoacyl (A)-site, the peptidyl (P)-site and the exit (E)-site tRNAs. In each site the tRNA anticodon loops interact with the small subunit and the tRNA acceptor stems interact with the large one.

Being the main player in this fundamental process, ribosomes are targeted by clinically relevant antibiotics [1–5]. The recently determined high-resolution structures of ribosomal particles [6–9], and of their complexes with over two dozen different antibiotics [10–19], has paved the way for a detailed examination of specific binding modes, leading to a better understanding of drug selectivity and the principles of drug resistance. This newly available information has shown that, although ribosomes theoretically offer multiple binding opportunities, all antibiotics bind at a single or a few sites. Most antibiotics interact primarily with rRNA and cause minor conformational changes; however, some antibiotics induce considerable local or allosteric conformational alterations, and some also interact with ribosomal proteins.

Diverse modes of antibiotic action have been identified, including miscoding, mobility minimizing, interference with substrate binding at the decoding center and at the PTC, and blockage of the protein exit tunnel. Noteworthy are the similarities in the interactions of edeine, pactamycin and the primary site of tetracycline with the small ribosomal subunit from *Thermus thermophilus* (T30S) [10–12], which have been elucidated by two independent laboratories. The use of clinically relevant drug concentrations and the consistency of these locations with resistance data manifest the reliability of the crystallographic results and suggest that dissimilarities observed in the crystal structures reflect phylogenetic or functional variability. In this article, we discuss lessons learned from the current structural findings (Box 1), focusing on unanswered questions and controversial issues.

Antibiotic selectivity is imperative for effective clinical use

All ribosomes show great structural and functional similarities. Nevertheless, a few subtle, albeit vital, differences between prokaryotic and eukaryotic ribosomes facilitate selectivity in antibiotic action, thereby enabling the therapeutic use of these drugs. The availability of structures of antibiotics bound to the large ribosomal subunit from the eubacterium *Deinococcus radiodurans* (D50S) [13,14,17–19] and to that of the archaeon *Haloarcula marismortui* (H50S) [15,16], which possess typical eukaryotic elements at the principal antibiotic target sites, provides a unique tool for investigating the principles of selectivity.

Implications of tunnel blockage for selectivity and resistance

Macrolides and ketolides have the highest clinical use. They function by blocking the exit tunnel for nascent proteins, thereby arresting protein elongation. The macrolide and ketolide antibiotic family consists of natural or semisynthetic compounds with a lactone ring to which one or two sugars are attached (Figure 1a). All of the crystal structures of complexes between macrolides or ketolides and large subunits that are currently available [13–19] show binding modes based on interactions of the lactone ring and the desosamine aminosugar predominantly with

Corresponding author: Ada Yonath (ada.yonath@weizmann.ac.il).
Available online 30 September 2004

 0167-7799/$ - see front matter doi:10.1016/j.tibtech.2004.09.006

Box 1. Take home lessons and future expectations

High-resolution structures of antibiotics bound to ribosomal particles show that antibiotics target functionally relevant locations in the ribosome such as the peptidyl transferase center (targeted by chloramphenicol and streptogramins A) and a high-affinity pocket in the tunnel along which nascent proteins progress (targeted by macrolides, ketolides and streptogramins B). Comparisons of the high-resolution crystal structures of ribosomal subunits from a eubacterium resembling pathogens (*Deinococcus radiodurans*) and an archaeon that shares properties with eukaryotes *(Haloarcula marismortui)* have deciphered subtle differences in these locations, despite their conservation. These minute differences lead to drug selectivity, thereby facilitating clinical use. An additional property that contributes to drug selectivity relates to relative drug quantities. Notably, clinically relevant concentrations were found to be sufficient for obtaining stoichiometric complexes of the prokaryotic pathogen model *D. radiodurans,* whereas crystallographically detectable binding of antibiotics to *H. marismortui* ribosomes were achieved only when extremely high amounts of drug were used.

The high-resolution structures also show that, despite apparent similarity in the binding modes of antibiotics exhibiting close or even indistinguishable modes of action, the chemical properties of a drug govern its exact interactions, thereby leading to variability in binding modes. Similarly, variations in drug properties seem to govern the exact nature of seemingly identical mechanisms of drug resistance. The observed variability in binding modes justifies expectations for improving antibiotic properties through the chemical modifications of existing compounds, as well as through the design of novel drugs on the basis of structural information.

The benefit from structural studies of antibiotic complexes extends beyond the clinical or drug design aspects, because the antibiotics bind mainly to ribosomal features with functional relevance. Thus, the emerging structural information greatly assists the elucidation of ribosomal mechanisms. Examples of new ribosomal properties and tasks that have been either revealed or reinforced by crystallographic studies include decoding (paromomycin), mRNA progression (spectinomycin and edeine), A-site binding to the small (tetracycline) and the large (chloramphenicol) subunits, PTC mobility (sparsomycin), tRNA rotatory motion (Synercid®) and tunnel gating (troleandomycin).

a structural pocket bordered by nucleotides A2058 and A2059 (*Escherichia coli* numbering is used throughout) of domain V of the 23S subunit (Figure 1a,b). The second macrolide sugar (cladinose) interacts directly with the ribosome only in a few cases [14,17].

Exceptional consistency in binding to the macrolide pocket has been observed for three closely related 14-membered macrolides, erythromycin and its semisynthetic derivatives, clarithromycin and roxithromycin [13]. Because this group was the first to be studied crystallographically, expectations were raised for comparable similarity in the binding modes of, and resistance mechanisms to all macrolides. Subsequent studies have shown, however, that although all macrolides bind to the same pocket, their orientations and interactions might vary in accordance with their chemical nature (Figure 1a–e).

The erythromycin binding mode indicates that increased bulkiness at position 2058 should impose spatial constrains and hamper macrolide binding. This nucleotide has a key role in macrolide selectivity. Thus, instead of the typical eubacterial adenine at position 2058, eukaryotes and most archaea, including *H. marismortui*, possess guanine in this position and do not bind 14-membered macrolides. Nucleotide 2058 is also the main factor in the two prominent mechanisms of resistance to macrolides, lincosamides and streptogramin$_B$ – namely, methylation of the *erm* gene and substitution of adenine to guanine [20,21]. In both mechanisms, the increased size at position 2058 eliminates interactions with the desosamine sugar.

Consistent with biochemical results [22,23], crystal structures of ribosomal complexes of ketolides and of 16-membered ring macrolides [14,15,18], which are designed to combat resistance by the addition of rather long extensions, have revealed additional drug interactions with domain II, which lines the tunnel wall approximately across domain V (Figure 1a). It is likely that these additional drug interactions compensate for the loss of the seemingly vital contacts of the desosamine sugar with A2058. Common to the binding modes of the three 16-membered macrolides, tylosin, carbomycin and spiramycin, is their location in the tunnel [15], which should lead to partial tunnel blockage (Figure 1b). Despite the similar location, variations have been observed in the global orientations of these 16-membered macrolides, including in the conformations of their lactone ring.

The 15-membered macrolide azithromycin seems to possess increased conformational flexibility, which it exploits in its binding modes to D50S [14] and H50S [15], which both differ from the binding mode of erythromycin [13]. In D50S, azithromycin binds cooperatively at two sites, which are both perpendicular to the tunnel direction, that stretch from the typical erythromycin pocket to domain II (Figure 1c). Consequently, azithromycin occupies most of the free space in the tunnel, consistent with its high efficiency and prolonged action [24].

Superficially, antibiotic binding to ribosomes with guanine at 2058 might indicate lower selectivity, which should consequently reduce clinical use of the drug. The wide use of azithromycin indicates the contrary and can be explained by comparing the modes of azithromycin binding to D50S and to H50S. As seen in Figure 1c, azithromycin binding to H50S blocks only a small part of the tunnel, whereas in D50S even the single azithromycin molecule that occupies the common macrolide binding mode (AZI-1 in Figure 1c) leads to effective blockage of the exit tunnel. This could be due to additional differences in the fine structures of prokaryotes and eukaryotes in the local environment of the macrolide binding pocket, as observed in the PTC [8]. Furthermore, it accords with the typical requirement for a remarkable excess of antibiotics for obtaining meaningful binding to H50S, indicating low affinity.

In troleandomycin, a 14-membered macrolide, all hydroxyl groups are either methylated or acetylated (Figure 1d), hence this drug cannot create the typical hydrogen bonds of macrolides. Nevertheless, it binds to the typical macrolide-binding pocket at nucleotide 2058, albeit in a different way compared with the binding of erythromycin and the ketolides (Figure 1d), demonstrating that functionally meaningful interactions with A2058 can involve various chemical moieties. Owing to the

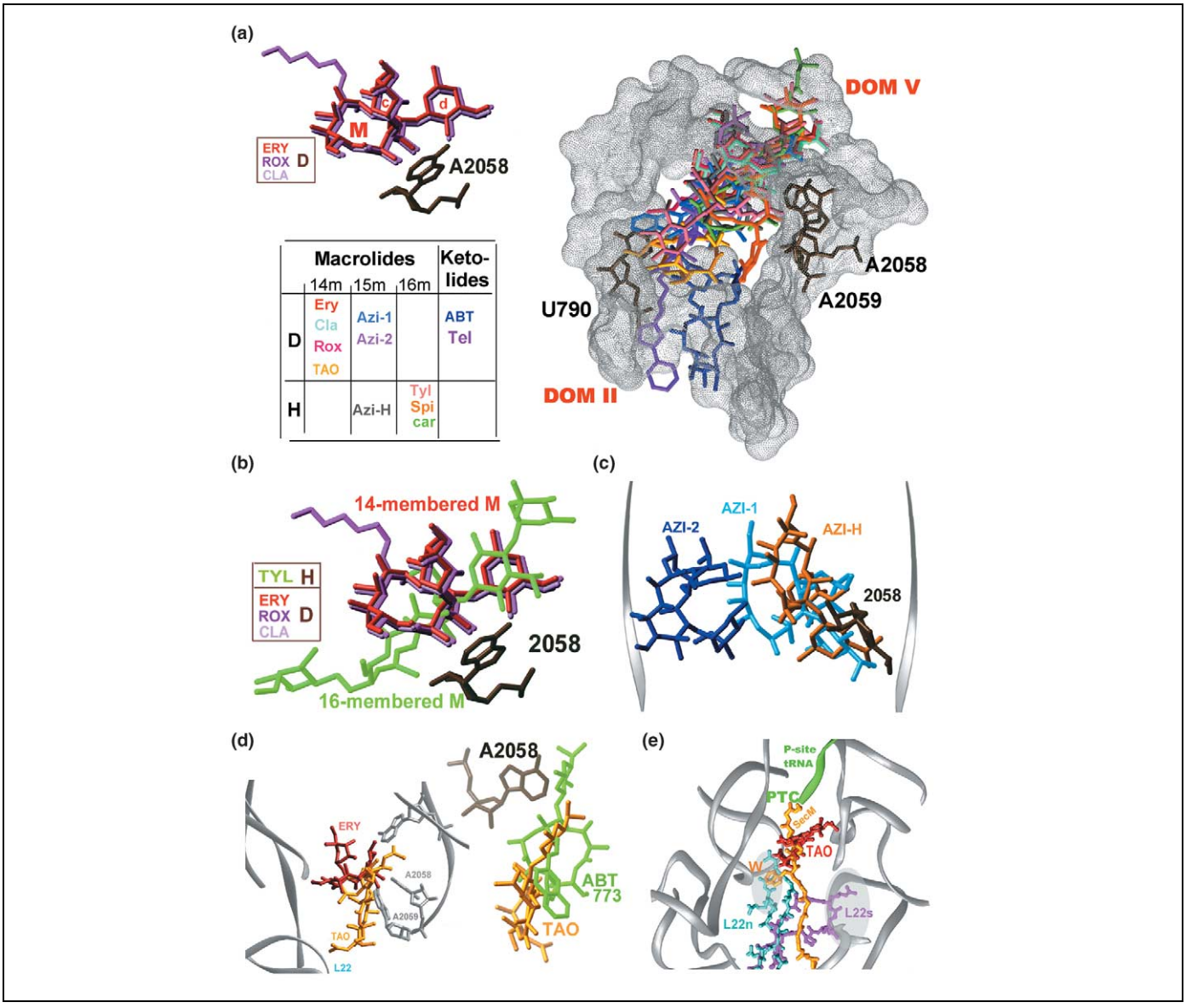

Figure 1. Macrolides and ketolides in the ribosome tunnel. **(a)** Principles of macrolides chemistry and the common binding modes of erythromycin (Ery), clarithromycin (Cla) and roxithromycin (Rox) to the protein exit tunnel of D50S, the large ribosomal subunit from *Deinococcus radiodurans*. Left, superposition of the locations of three 14-membered macrolides in D50S, and the location of A2058, the key nucleotide for binding, selectivity and resistance. The main macrolides components, namely the macrolactone ring and the desosamine and cladinose sugars, are marked by M, d and c, respectively. Right, binding modes of several antibiotics within a cross-section of the ribosomal tunnel (dotted gray cloud) at the level of the macrolides-binding pocket. The positions of the key nucleotides for macrolide or ketolide binding, selectivity and resistance in domains V (DOM V) and II (DOM II) are marked. For orientation, the approximate position of the peptidyl transferase center (PTC) is on top. The 14-, 15- and 16-membered macrolactone ring compounds (14m, 15m and 16m, respectively) with the color code of the different antibiotics are shown in the table. The ribosomes sources are indicated by H (H50S, the large ribosomal subunit from *Haloarcula marismortui*) and D (D50S). Abbreviations: TAO, troleandomycin; Azi, azithromycin (Azi-1 and Azi-2: primary and secondary azithromycin sites in D50S); Azi-H, azithromycin site in H50S; ABT, ABT-773; Tel, telithromycin; Tyl, tylosin, Spi, spiramycin; Car, carbomycin. **(b)** Superposition of the location of the 16-membered macrolide tylosin bound to H50S on the locations of the three 14-membered macrolides bound to D50S shown in (a), indicating that tylosin binding to tunnels with G (guanine) instead of A (adenosine) at position 2058, should not severely hamper nascent protein passage. **(c)** Superposition of azithromycin bound to H50S (AZI-H) and D50S (AZI-1 and AZI-2), together with the position of A2058 and the approximate boundary of the ribosome tunnel (gray ribbons). This figure shows that azithromycin binding to D50S, which, similar to typical eubacterial pathogens, possesses A in position 2058, should arrest nascent protein passage even when its secondary site is not occupied. However, azithromycin binding to H50S, which has G instead of A at position 2058 (the crucial nucleotide for antibiotics selectivity), should not severely hamper nascent protein passage, thereby explaining drug selectivity. **(d)** Troleandomycin (TAO)-binding mode (left), compared with those of erythromycin and ABT-773 (right). In both views, the main axis of the tunnel points downwards. The two views are shown from opposite tunnel sides. Reproduced with permission from Ref. [40]. **(e)** View into the tunnel (gray), showing the troleandomycin (red) induced swinging [swinging conformation (L22n) is shown in magenta] of the β-hairpin tip [native orientation (L22n) is shown in cyan] of protein L22. The modeled polypeptide chain (yellow) represents a nascent protein containing the sequence motif known to cause secretion monitor (SecM) elongation arrest. This motif (sequence X_5-W-X_{10}-P, where X is any amino acid and proline is the last amino acid to be incorporated into the nascent chain) is located about 150 residues from the N terminus. The gray shaded areas show the approximate locations of the mutations that alleviate the elongation arrest [25]. The position of the tryptophan (W) essential for elongation arrest is also shown to indicate the stunning correlation between it and that of troleandomycin. When incorporated into the protein, the SecM proline required for the arrest is the top amino acid of the modeled nascent chain and located at the PTC, namely the position of the end of the P-site tRNA (green).

bulkiness of its substituents and its larger size, the lactone ring of troleandomycin is inclined to the tunnel wall, rather than being perpendicular to it, and thus reaches domain II [17], causing the β-hairpin tip of the protein L22 to swing across the tunnel (Figure 1e). The interactions of the L22 β-hairpin tip can be correlated with mutations that bypass tunnel arrest [25], thereby validating biochemical evidence for the conformational dynamics of the

tunnel and its participation in gating and sequence discrimination [25–27].

Selectivity and variability in PTC targeting

A universal, sizable symmetry-related region, which connects all ribosomal functional centers involved in amino acid polymerization, facilitates the smooth and efficient formation of peptide bonds [28–30]. The link between this unique architectural design and substrate positioning suggests that translocation involves a rotatory motion of the tRNA 3′ end that is synchronized with the overall shift in mRNA and tRNA. Guided by PTC components, which create its exact pattern, this rotatory motion results in stereochemistry suitable for peptide bond formation and for directing nascent proteins into their exit tunnel. Consistently, crystal structures of functional complexes of D50S have confirmed that the ribosome is a ribozyme that provides positional rather than chemical catalysis, and have indicated that precise placement of the tRNA is crucial for amino acid polymerization [28–30].

A2602 and U2585, two universally conserved nucleotides that are positioned at the PTC center [28–30], facilitate and anchor the rotatory motion (Figure 2a). Some antibiotics target A2602 and U2585, highlighting the crucial roles of these two nucleotides. Sparsomycin is a potent universal ribosomal inhibitor that binds to A2602 [16,28,31]. On entering a non-occupied large subunit, it stacks against this most flexible nucleotide, and causes marked conformational alterations in the whole PTC. These alterations, in turn, influence positioning of the A-site tRNA [28,31,32], which explains why sparsomycin was originally considered to be an A-site inhibitor although it does not interfere with A-site substrates. Because it stacks to A2602 on the side facing the P-site (Figure 2b), sparsomycin can also enhance the binding of non-productive tRNAs [33]. Conversely, when sparsomycin enters the large subunit simultaneously with a P-site substrate analog, it causes only a modest conformational alteration in A2602. Because in this situation the P-site is occupied by the analog, sparsomycin stacking against A2602 seems to face the A-site [16] (Figure 2c), indicating that there is a significant correlation between the mode of antibiotic binding and the functional state of the ribosome [32].

U2585 is targeted by streptogramins, a family of antimicrobial drugs in which each antibiotic consists of two synergistic components (S_A and S_B) that cooperatively convert weak bacteriostatic effects into lethal bactericidal activity. In crystals of the D50S–Synercid® complex, obtained at clinically relevant drug concentrations, the S_A component dalfopristin binds to the PTC and induces marked conformational alterations, including a flip of the U2585 base (Figure 2d,e). In this way, the S_A component paralyzes the ability of U2585 to anchor the rotatory motion [34]. Because this motion makes a crucial contribution to cell vitality, it is likely that the processivity of protein biosynthesis will attempt to recover the correct positioning of U2585 and either expel or relocate S_A, consistent with the low antibacterial effect of this component. The S_B component of Synercid®, quinupristin, is located in the common macrolide pocket and interacts with A2058. In comparison to erythromycin [13], quinupristin is slightly inclined owing to its bulky structure [19], rationalizing its reduced antibacterial effects. When bound simultaneously both Synercid® components interact with each other, however, stabilizing the flipped confirmation of U2585 and thereby enhancing the overall antimicrobial activity.

In the complex of H50S and the S_A-like component Virginiamycin-M, the U2585 conformation is hardly altered (Figure 2f) [16]. This mild drug action can be explained by the different conformation of the PTC of H50S as compared with the PTC of eubacterial ribosomes [8,35], consistent with the inability of the PTC of H50S to bind chloramphenicol [16], a known A-site competitor [36–38]. Furthermore, although footprinting experiments have indicated that S_B binds to the archaeon *Halobacterium halobium* [39], no binding of S_B to H50S was detected in this complex [16]. This apparent contradiction can be explained by weak or low-level S_B binding, which is insufficient for crystallographic detection, which requires close to quantitative binding. Indeed, a lack of S_B interactions with H50S is not surprising because, on the basis of the structure of the D50S complex, it requires interactions with an adenine at position 2058.

The two different chloramphenicol-binding sites that have been observed crystallographically demonstrate the interplay between structural and clinical implications, and illuminate the distinction between medically meaningful and less relevant binding. This PTC-targeting antibiotic attacks eubacteria, with a considerable toxicity in humans. Its complex with D50S, obtained by using clinically relevant drug concentrations [13], shows that chloramphenicol is located in the A-site (Figure 2b,g), consistent with most of the biochemical and resistance data [36–38]. By contrast, chloramphenicol binding to *H. marismortui* necessitates extremely high drug concentrations, similar to those of other ribosome-targeting antibiotics (up to 1000 times more than the concentrations used commonly in therapeutic treatment). Notably, even at these outstandingly high levels of chloramphenicol, no binding at the PTC A-site was detected in the H50S complex. Thus, no structural basis for the prominent A-site binding competition could be implied. Instead, another site was found at the entrance to the ribosomal tunnel [16]. Figure 2g shows that such binding should have marginal or no clinical significance, because in this position chloramphenicol does not interfere with peptide bond formation or with nascent chain progression. Furthermore, although superposition of the chloramphenicol-binding site of H50S onto the D50S structure might implicate competition between chloramphenicol and macrolides, in *H. marismortui* such competition is meaningless because H50S does not bind the common macrolides because it possesses a guanine rather than an adenine at position 2508.

The lack of chloramphenicol binding to the A-site in the PTC of H50S could result from inherent conformational differences between archaea and eubacteria [8,35]. It could also be due to the composition of the solution in the H50S crystals, which barely resembles the *H. marismortui*

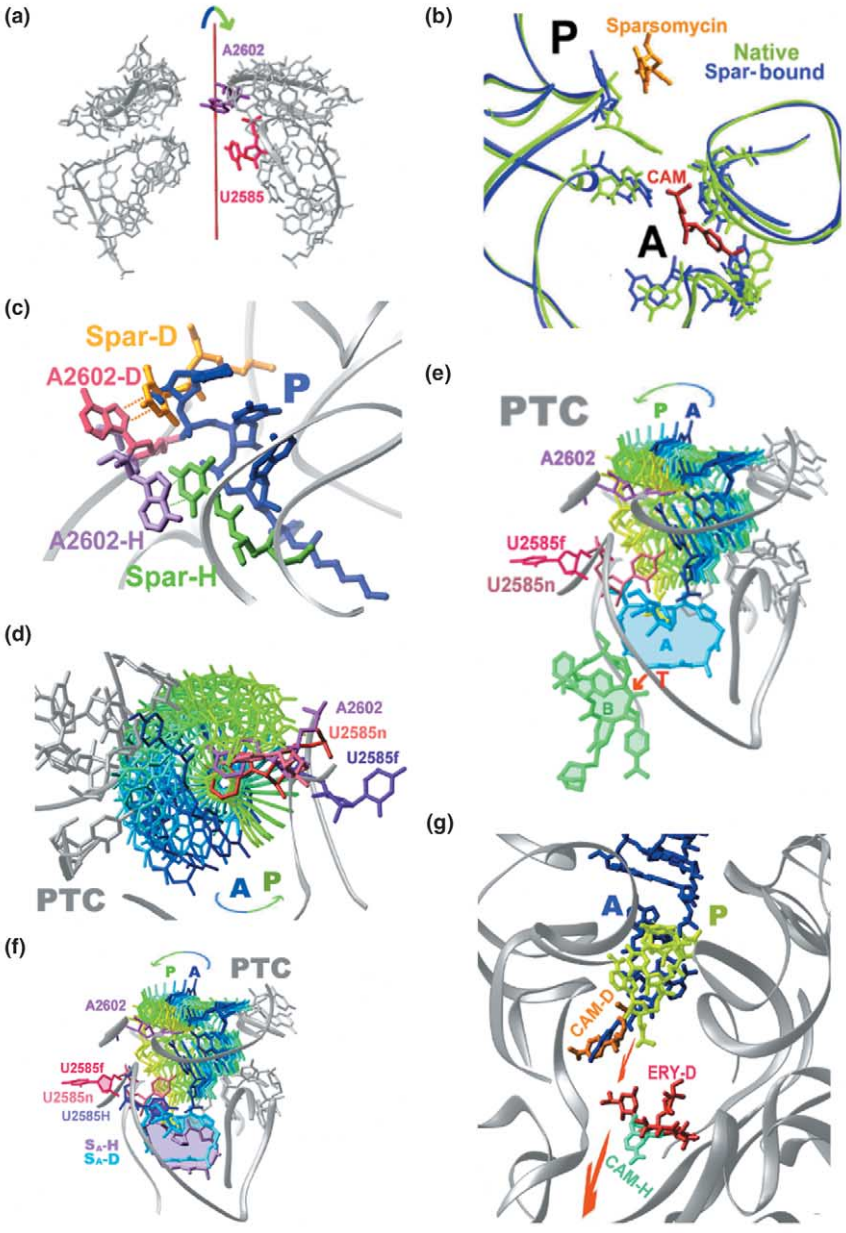

Figure 2. Peptidyl-transferase center (PTC) antibiotics: mobility and synergism. **(a)** Side view of the peptidyl transferase center (PTC) in the large ribosomal subunit from *Deinococcus radiodurans* (D50S), showing the positions of the two conserved flexible nucleotides, A2602 (which interacts with the tRNA 3′ end near its connection to the helical part of the tRNA) and U2585 (which interacts with the amino acid), that facilitate and anchor the rotatory motion of the A-site tRNA into the P-site, in the direction of the arrow. The symmetry axis is shown in red. Reproduced with permission from Ref. [34]. **(b)** Locations of chloramphenicol (CAM) at the PTC A-site in D50S and sparsomycin (Spar), which stacks to A2602. The 180° flip of this base and the alterations caused by sparsomycin binding in the whole PTC (indicated in blue as opposed to the native structure indicated in green) explain how sparsomycin can compete with A-site binding, even though it is located in the middle of the PTC. **(c)** Sparsomycin-binding sites in D50S (Spar-D) and H50S (Spar-H), the large ribosomal subunit from *Haloarcula marismortui*, highlighting the marked difference in binding mode that originates from with the ribosomal functional state. The position of the P-site substrate analog, as seen in the structure of its complex with H50S and sparsomycin[16], explains how sparsomycin stabilizes non-productive P-site tRNA binding. **(d)** View from the tunnel towards the PTC, perpendicular to the view in (a), showing the rotatory motion (indicated by the round arrow) of the A-site tRNA 3′ end from the A-site (blue) to the P-site (green). The PTC boundaries that delineate the path of the rotatory motion are shown in gray. The rotatory motion is represented by the gradual transfer from blue to green. Shown are snapshots of the rotatory motion, obtained by successive 15° rotations of the rotating moiety around the bond connecting the 3′ end with the rest of the tRNA molecule captured using a 35-nucleotide compound that mimics the A-site tRNA acceptor stem and its aminoacylated 3′ end as an A-site analog. The conformational alteration of U2585 (U2585f) induced by the binding of dalfopristin, the S_A component of Synercid®, is shown in comparison to its native orientation (U2585n). Reproduced with permission from Ref. [34]. **(e)** View perpendicular to that shown in (d), together with both Synercid® compounds represented by A (dalfopristin) and B (quinupristin), indicating the way in which these two components function in synergy to enhance antibiotic action. T indicates the tunnel entrance. Reproduced with permission from Ref. [40]. **(f)** Same view as in (e), but without the snapshots indicating the rotatory motion. The A-site (A) and the derived P-site (P) tRNA [28] are shown, as well as the position of U2585 in H50S and D50S. Note the modest alteration of U2585 in H50S. Reproduced with permission from Ref. [40]. **(g)** View of the PTC and the tunnel entrance (gray ribbons), showing the positions of chloramphenicol primary binding site, as seen in D50S (CAM-D), and its secondary positions, as detected only in H50S (CAM-H). A-site (A) tRNA and the derived P-site (P) tRNA [28] are included to highlight the known competition between chloramphenicol and A-site tRNA. The erythromycin site in D50S (ERY-D) is included because the position of CAM in H50S (CAM-H) overlaps its location. Note that the size of CAM is not sufficient for efficient tunnel blockage. Orange arrows indicate the direction of the nascent protein progression.

environment *in situ* [8,40], especially with regard to the ratios between monovalent and divalent ions. Such variations have been shown to lead to significant conformational alterations in the PTC [41,42], thereby reducing the efficiency of tRNA binding to the A-site [43]. Because tRNA binding to the A-site is the ribosomal function known to be targeted by chloramphenicol, it is conceivable that under these conditions the affinity of chloramphenicol for the A-site is also reduced.

Open issues

So far, most biochemical and genetics studies have been done on the *E. coli* ribosome, despite its inherent instability and complex genome. These studies have yielded both valuable information and questionable conclusions, such as the interaction between macrolides and domain II [21,44]. Organisms such as *H. halobium*, which have been used in more recent studies because they possess a single chromosomal copy of the rRNA operon [36], have resolved several ambiguities but can also provide misleading results, as in the case of sparsomycin binding [45].

E. coli is also the organism that has revealed that mutations in proteins L4 and L22 render resistance to erythromycin [46,47]. Although no interactions were detected between erythromycin and these proteins in D50S(13), the crystal structure of the mutated L22 protein [48], combined with cryo-electron microscopy studies [49] and three-dimensional information from the D50S–erythromycin structure [13], has led to sound proposals that the drug functions indirectly by perturbing the conformation of rRNA, consistent with the results of RNA probing studies [50].

In addition, the suitability of *E. coli* as a pathogen model despite its phylogenetic diversity has been shown by the similarity of the ratios of the minimal inhibitory concentration (MIC), required for ABT-773, erythromycin and troleandomycin action on *E. coli* and *Pseudomonas aeroginosa* (1, 4 and 8, respectively; T.A. unpublished). It therefore seems that, despite phylogenetic diversity, model bacteria, such as *E. coli, D. radiodurans, H. Halobium* and *M. smegmatis* [51] can lead to useful information, provided that extreme care is taken when relying solely on a single method.

X-ray crystallography is a powerful method for elucidating binding details at the molecular level. Because so far no well-diffracting crystals have been obtained for ribosomes from pathogens, studies are confined to the currently available crystals. The eubacteria *T. thermophilus* and *D. radiodurans* resemble pathogens and thus can be considered as suitable pathogen models. Nevertheless, the specific binding modes of two antibiotics, azithromycin and troleandomycin (see above), have stimulated considerable concern. Modeling and energetic considerations have indicated, however, the feasibility that azithromycin binds to two sites in the ribosomes of several pathogens, such as *Haemophilus influenzae, Mycobacterium tuberculosis, Helicobacter pylori, Mycoplasma pneumoniae* and *Mycobacterium leprae* [34].

Similarly, the interactions of troleandomycin with *D. radiodurans*, which deviate from the binding mode of erythromycin, clarithromycin and roxithromycin [13], have been verified biochemically (D. Baram *et al.*, unpublished). Contrary to *D. radiodurans*, the information obtained for *H. marismortui* ribosomes is restricted owing to experimental reasons. Thus, the high salinity (~2 M NaCl) within H50S crystals [9] is far from the environmental conditions within the cells of pathogenic bacteria. Nevertheless, because *H. marismortui* resembles eukaryotes with respect to the nucleotide at position 2058 and the A-site of the PTC – the key factors involved in macrolide and chloramphenicol binding – the complexes of H50S with antibiotics are useful for highlighting principles of drug selectivity.

Another open issue is the influence of the chemical properties and conformational flexibility of the antibiotics on their binding modes and the mechanisms of resistance to them. For example, both troleandomycin and the ketolides are 14-membered macrolides, both bind at the 2058 pocket, both interact with domain II, both have the same MICs values (for *D. radiodurans*) and both have been shown to induce a similar resistant mutant (T.A., D. Baram and I. Shalit, unpublished). Nevertheless, the ketolides and troleandomycin show significantly different binding patterns (Figure 1d), originating from their specific chemical and geometrical properties. It seems, therefore, that comparable interactions observed for different and similar antibiotics might or might not result from comparable drug orientations. Likewise, because resistance could originate from the disruption of various interactions, a specific mutation leading to resistance to several antibiotics does not necessarily imply that all of these antibiotics have the same binding mode.

Conclusions

The ribosome possesses pockets of functional significance that attract antibiotics. Among them are the decoding center, the exit tunnel, the PTC and the anchors of the A-site to P-site rotatory motion. The nature of ribosome–antibiotic interactions is dominated by both the chemical properties of the drugs and the specific conformation of the ribosomal pocket, which in turn is governed by the functional state of the ribosome and by phylogenetic and environmental factors. Thus, the binding of similar antibiotics to a specific pocket does not imply similar interactions of the bound drug, because a single pocket might form various types of interaction. The variability in binding modes of slightly or radically modified antibiotics, observed in the high-resolution structures of ribosome–antibiotic complexes, justifies expectations for the design of improved antibiotic properties.

Acknowledgements

We thank I. Shalit and all members of the ribosome groups at the Max Planck Society and the Weizmann Institute. X-ray diffraction data were collected at the ID19/SBC/APS/ANL and ID14/ESRF-EMBL beamlines. The US National Institutes of Health (grant GM34360), the Human Frontier Science Program Organization (grant RGP0076/2003) and the Kimmelman Center for Macromolecular Assemblies provided support. A.Y. holds the Martin and Helen Kimmel Professorial Chair.

References

1 Vazquez, D. (1979) Inhibitors of protein biosynthesis. *Mol. Biol. Biochem. Biophys.* 30, 1–312

2 Gale, E.F. *et al*. (1981) *The Molecular Basis of Antibiotic Action*, John Wiley & Sons
3 Cundliffe, E. (1981) *Antibiotic Inhibitors of Ribosome Function*, John Wiley & Sons
4 Spahn, C.M. and Prescott, C.D. (1996) Throwing a spanner in the works: antibiotics and the translation apparatus. *J. Mol. Med.* 74, 423–439
5 Auerbach, T. *et al*. (2002) Antibiotics targeting ribosomes: crystallographic studies. *Curr. Drug Targets Infect. Disord.* 2, 169–186
6 Schluenzen, F. *et al*. (2000) Structure of functionally activated small ribosomal subunit at 3.3 angstroms resolution. *Cell* 102, 615–623
7 Wimberly, B.T. *et al*. (2000) Structure of the 30S ribosomal subunit. *Nature* 407, 327–339
8 Harms, J. *et al*. (2001) High resolution structure of the large ribosomal subunit from a mesophilic eubacterium. *Cell* 107, 679–688
9 Ban, N. *et al*. (2000) The complete atomic structure of the large ribosomal subunit at 2.4 Å resolution. *Science* 289, 905–920
10 Carter, A.P. *et al*. (2000) Functional insights from the structure of the 30S ribosomal subunit and its interactions with antibiotics. *Nature* 407, 340–348
11 Brodersen, D.E. *et al*. (2000) The structural basis for the action of the antibiotics tetracycline, pactamycin, and hygromycin B on the 30S ribosomal subunit. *Cell* 103, 1143–1154
12 Pioletti, M. *et al*. (2001) Crystal structures of complexes of the small ribosomal subunit with tetracycline, edeine and IF3. *EMBO J.* 20, 1829–1839
13 Schluenzen, F. *et al*. (2001) Structural basis for the interaction of antibiotics with the peptidyl transferase centre in eubacteria. *Nature* 413, 814–821
14 Schluenzen, F. *et al*. (2003) Structural basis for the antibiotic activity of ketolides and azalides. *Structure* 11, 329–338
15 Hansen, J.L. *et al*. (2002) The structures of four macrolide antibiotics bound to the large ribosomal subunit. *Mol. Cell* 10, 117–128
16 Hansen, J.L. *et al*. (2003) Structures of five antibiotics bound at the peptidyl transferase center of the large ribosomal subunit. *J. Mol. Biol.* 330, 1061–1075
17 Berisio, R. *et al*. (2003) Structural insight into the role of the ribosomal tunnel in cellular regulation. *Nat. Struct. Biol.* 10, 366–370
18 Berisio, R. *et al*. (2003) Structural insight into the antibiotic action of telithromycin against resistant mutants. *J. Bacteriol.* 185, 4276–4279
19 Harms, J. *et al*. (2004) Alterations at the peptidyl transferase centre of the ribosome induced by the synergistic action of the streptogramins dalfopristin and quinupristin. *BMC Biol.* 2, 4
20 Weisblum, B. (1995) Erythromycin resistance by ribosome modification. *Antimicrob. Agents Chemother.* 39, 577–585
21 Douthwaite, S. *et al*. (2000) Macrolide-ketolide inhibition of MLS-resistant ribosomes is improved by alternative drug interaction with domain II of 23S rRNA. *Mol. Microbiol.* 36, 183–193
22 Xiong, L. *et al*. (1999) A ketolide resistance mutation in domain II of 23S rRNA reveals the proximity of hairpin 35 to the peptidyl transferase centre. *Mol. Microbiol.* 31, 633–639
23 Hansen, L.H. *et al*. (1999) The macrolide–ketolide antibiotic binding site is formed by structures in domains II and V of 23S ribosomal RNA. *Mol. Microbiol.* 31, 623–631
24 Alvarez-Elcoro, S. and Enzler, M.J. (1999) The macrolides: erythromycin, clarithromycin, and azithromycin. *Mayo Clin. Proc.* 74, 613–634
25 Nakatogawa, H. and Ito, K. (2002) The ribosome exit tunnel functions as a discriminating gate. *Cell* 108, 629–636
26 Gong, F. and Yanofsky, C. (2002) Instruction of translating ribosome by nascent peptide. *Science* 297, 1864–1867
27 Woolhead, C.A. *et al*. (2004) Nascent membrane and secretory proteins differ in FRET-detected folding far inside the ribosome and in their exposure to ribosomal proteins. *Cell* 116, 725–736
28 Bashan, A. *et al*. (2003) Structural basis of the ribosomal machinery for peptide bond formation, translocation, and nascent chain progression. *Mol. Cell* 11, 91–102
29 Bashan, A. *et al*. (2003) Ribosomal crystallography: peptide bond formation and its inhibition. *Biopolymers* 70, 19–41
30 Agmon, I. *et al*. (2003) On peptide bond formation, translocation, nascent protein progression and the regulatory properties of ribosomes. *Eur. J. Biochem.* 270, 2543–2556
31 Porse, B.T. *et al*. (1999) Direct crosslinking of the antitumor antibiotic sparsomycin, and its derivatives, to A2602 in the peptidyl transferase center of 23S-like rRNA within ribosome–tRNA complexes. *Proc. Natl. Acad. Sci. U. S. A.* 96, 9003–9008
32 Goldberg, I.H. and Mitsugi, K. (1966) Sparsomycin, an inhibitor of aminoacyl transfer to polypeptide. *Biochem. Biophys. Res. Commun.* 23, 453–459
33 Monro, R.E. *et al*. (1969) Action of sparsomycin on ribosome-catalysed peptidyl transfer. *Nature* 222, 356–358
34 Agmon, I. *et al*. (2004) Ribosomal crystallography: a flexible nucleotide anchoring tRNA translocation, facilitates peptide-bond formation, chirality discrimination and antibiotics synergism. *FEBS Lett.* 567, 20–26
35 Yusupov, M.M. *et al*. (2001) Crystal structure of the ribosome at 5.5 Å resolution. *Science* 292, 883–896
36 Mankin, A.S. and Garrett, R.A. (1991) Chloramphenicol resistance mutations in the single 23S rRNA gene of the archaeon *Halobacterium halobium*. *J. Bacteriol.* 173, 3559–3563
37 Izard, T. and Ellis, J. (2000) The crystal structures of chloramphenicol phosphotransferase reveal a novel inactivation mechanism. *EMBO J.* 19, 2690–2700
38 Shaw, W.V. and Leslie, A.G. (1991) Chloramphenicol acetyltransferase. *Annu. Rev. Biophys. Biophys. Chem.* 20, 363–386
39 Porse, B.T. and Garrett, R.A. (1999) Sites of interaction of streptogramin A and B antibiotics in the peptidyl transferase loop of 23S rRNA and the synergism of their inhibitory mechanisms. *J. Mol. Biol.* 286, 375–387
40 Yonath, A. (2002) The search and its outcome: high-resolution structures of ribosomal particles from mesophilic, thermophilic, and halophilic bacteria at various functional states. *Annu. Rev. Biophys. Biomol. Struct.* 31, 257–273
41 Zamir, A. *et al*. (1974) The inactivation and reactivation of *Escherichia coli* ribosomes. *Methods Enzymol.* 30, 406–426
42 Bayfield, M.A. *et al*. (2001) A conformational change in the ribosomal peptidyl transferase center upon active/inactive transition. *Proc. Natl. Acad. Sci. U. S. A.* 98, 10096–10101
43 Moore, P.B. and Steitz, T.A. (2003) After the ribosome structures: how does peptidyl transferase work? *RNA* 9, 155–159
44 Vester, B. and Douthwaite, S. (2001) Macrolide resistance conferred by base substitutions in 23S rRNA. *Antimicrob. Agents Chemother.* 45, 1–12
45 Tan, G.T. *et al*. (1996) Mutations in the peptidyl transferase center of 23S rRNA reveal the site of action of sparsomycin, a universal inhibitor of translation. *J. Mol. Biol.* 261, 222–230
46 Wittmann, H.G. *et al*. (1973) Biochemical and genetic studies on two different types of erythromycin resistant mutants of *Escherichia coli* with altered ribosomal proteins. *Mol. Gen. Genet.* 127, 175–189
47 Chittum, H.S. and Champney, W.S. (1994) Ribosomal protein gene sequence changes in erythromycin-resistant mutants of *Escherichia coli*. *J. Bacteriol.* 176, 6192–6198
48 Davydova, N. *et al*. (2002) L22 ribosomal protein and effect of its mutation on ribosome resistance to erythromycin. *J. Mol. Biol.* 322, 635–644
49 Gabashvili, I.S. *et al*. (2001) The polypeptide tunnel system in the ribosome and its gating in erythromycin resistance mutants of L4 and L22. *Mol. Cell* 8, 181–188
50 Gregory, S.T. and Dahlberg, A.E. (1999) Erythromycin resistance mutations in ribosomal proteins L22 and L4 perturb the higher order structure of 23S ribosomal RNA. *J. Mol. Biol.* 289, 827–834
51 Bottger, E.C. *et al*. (2001) Structural basis for selectivity and toxicity of ribosomal antibiotics. *EMBO Rep 2* 318, 23